Age-Associated Activation of Epigenetically Repressed Genes in the Mouse

Pamela E. Bennett-Baker, Jodi Wilkowski and David T. Burke[1]

Department of Human Genetics, University of Michigan School of Medicine, Ann Arbor, Michigan 48109-0618

Manuscript received May 7, 2003
Accepted for publication August 18, 2003

ABSTRACT

Epigenetic control of gene expression is a consistent feature of differentiated mammalian cell types. Epigenetic expression patterns are mitotically heritable and are stably maintained in adult cells. However, unlike somatic DNA mutation, little is known about the occurrence of epigenetic change, or epimutation, during normal adult life. We have monitored the age-associated maintenance of two epigenetic systems—X inactivation and genomic imprinting—using the genes *Atp7a* and *Igf2*, respectively. Quantitative measurements of RNA transcripts from the inactive and active alleles were performed in mice from 2 to 24 months of age. For both genes, older animal cohorts showed reproducible increases in transcripts expressed from the silenced alleles. Loss of X chromosome silencing showed cohort mean increases of up to 2.2%, while imprinted-gene activation increased up to 6.7%. The results support the hypothesis that epigenetic loss of gene repression occurs in normal tissues and may be a contributing factor in progressive physiological dysfunction seen during mammalian aging. Quantitatively, the loss of epigenetic control may be one to two orders of magnitude greater than previously determined somatic DNA mutation.

DAMAGE to cellular information has been proposed to accumulate throughout life and to have an impact on the specificity and quality of physiological control (Szilard 1959; Holliday 1988; Johnson *et al.* 1999). In differentiated cells, the mitotically heritable information for gene regulation resides in both the genomic DNA sequence and epigenetic chromatin patterns (Weiler and Wakimoto 1995; Latham 1999). Direct DNA mutations and chromosomal aberrations are known to increase with age. However, cumulative lifetime base-pair mutations are observed at ~1 in 10,000–100,000 nucleotides in aging mice and humans (King *et al.* 1994; Martus *et al.* 1995). This infrequent occurrence of DNA-level damage contrasts with the extensive cell and tissue dysfunction seen in older individuals.

The cumulative loss of gene regulation over time—and over many genes—may lead to the failures in cellular and tissue function seen during aging. Since thousands of genes are epigenetically silenced in each differentiated cell type, the unintended activation of these genes is likely to increase the gene expression "noise" within the cell. Although complex network systems are buffered to small changes in the signal-to-noise ratio of information, large amounts of informational noise are likely to have pleiotropic and negative effects (McAdams and Arkin 1999; Becksei and Serrano 2000). While qualitative observations of mammalian epigenetic change during aging have been made (Cattanach 1974; Wareham *et al.* 1987), precise quantitative measurements of epigenetic maintenance are essential to assess its possible phenotypic impact.

In this report, we determine quantitative changes in epigenetic regulation in animals across normal life, using two well-studied mammalian epigenetic systems. Epigenetic regulation in aging mammals can be quantitatively measured using genes subject to X chromosome inactivation and genomic imprinting. In both regulatory systems, the two alleles of the gene are differentially expressed, with one homolog transcriptionally active and the other inactive. The inactive and active alleles (i) have an essentially identical genomic DNA sequence, (ii) coexist within a single cellular environment, (iii) are maintained in their activity states through mitosis, and (iv) produce mRNA transcripts of identical structure (Lyon 1999; Wolf and Jörn 2001). Therefore, the relative expression of the two allelic gene copies is primarily under the control of epigenetic mechanisms and can be quantitatively assessed by measuring steady-state ratios of the two allelic transcripts. Using this system as a sensitive monitor of epigenetic regulation, we have observed reproducible age-associated loss of stability in populations of laboratory mice held under controlled environmental conditions.

MATERIALS AND METHODS

Animal stocks and handling: The mouse translocation T(X;16)16H (abbreviated T16H) generates female animals having uniform inactivation of the normal (*i.e.*, nontranslocated) X chromosome (Eicher 1970). Two T16H stocks used in this study, although derived from the same initial translocation event, are genetically distinct, since they have been maintained as separate stocks (noninbred) at the Jackson Laboratory (JAX) and the Medical Research Council (MRC) Harwell

[1]*Corresponding author:* Department of Human Genetics, University of Michigan School of Medicine, 1241 E. Catherine St., Ann Arbor, MI 48109-0618. E-mail: dtburke@umich.edu

facility. Female T16H++/+*Eda*^{Ta}+ animals (obtained from JAX) were crossed to CBA/CaHN-*Btk*$^{xid/J}$ males (obtained from JAX) to produce the T16H++/++*Btk*$^{xid/J}$ (abbreviated J/X) population of T16H female mice. In a brother-sister mating scheme, male ++*Atp7a*$^{Mo\text{-}blo}$/Y animals (obtained from the MRC) were crossed with female T16H++/++*Eda*^{Ta} animals (obtained from the MRC) to produce the T16H++/++ *Atp 7a*$^{Mo\text{-}blo}$ (abbreviated T/M) population of T16H females. The BALB/cJ, C57BL/6J, and *Mus spretus* parents were obtained from the Jackson Laboratory and used to produce populations of F_1 hybrids: CB6F1 and C57BL/6J × *M. spretus* F_1. All experimental animals were bred and housed at the University of Michigan School of Medicine Unit for Laboratory Animal Medicine. All animals were fed *ad lib* and were killed at set time points to generate cohorts of aged mice. Tissues were dissected and frozen in liquid nitrogen for long-term storage at −80°.

RNA preparation, reverse transcription, and PCR: Total RNA was prepared from frozen whole tissues using TRIZOL reagent (GIBCO BRL, Gaithersburg, MD) as described by the manufacturer. Total RNA was DNaseI treated prior to reverse transcription (Ausubel *et al.* 1989). Reverse transcription was performed in a 20-μl reaction mixture containing 1 μg total RNA, 0.5 mm of each deoxynucleotide, 10 mm dithiothreitol, 50 mm Tris-HCl pH 8.2, 50 mm KCl, 6 mm $MgCl_2$, 0.05 mg/ml oligo$(dT)_{12\text{-}18}$ (Amersham Pharmacia Biotech), 1 unit RNase inhibitor (Boehringer Mannheim, Indianapolis), and 20 units avian myeloblastosis virus Super Reverse Transcriptase (Molecular Genetics Resources). Reactions were incubated for 5 min at room temperature followed by 1.5 hr at 42°.

Aliquots of cDNA products (1–2 μl) were amplified by the polymerase chain reaction (PCR). PCR primer sequences were as follows:

AF: 5′-AGCAGCACATTAGCAACTTCT-3′
AR: 5′-ACAGGAAACCTACGTATGACAA-3′
P1: 5′-GCAGGGACAGTTCCATCAGGTCC-3′
P2: 5′-CACACTAAGATCTCTCTGCTCCA-3′
P3: 5′-TGATTTTGCCAATTGTTTTTAAGC-3′

The X-linked ATPase copper-transporting type 7a (*Atp7a*) gene was amplified with primers AF and AR using standard PCR conditions. The insulin growth factor-2 (*Igf2*) gene was amplified with either P1 and P3 or P2 and P3 using step-down PCR conditions (Hecker and Roux 1996). The PCR products were purified by gel electrophoresis (Zhen and Swank 1993) or by treatment with ExoSAP-IT (United States Biochemical, Cleveland) as described by the manufacturer.

Allelic expression primer-extension assays: Primer-extension (PE) reactions were performed in 8-μl total volumes containing 100 fmol of an HPLC-purified, CY-5-labeled, oligonucleotide primer (Genosys, The Woodlands, TX), 25–100 fmol DNA template, 25 μm of each nucleotide needed for the differential extension, 2 mm $MgCl_2$, 10 mm Tris-HCl pH 8.8, 10 mm KCl, 0.002% Tween-20, and 0.64 units Thermo Sequenase (Amersham Pharmacia Biotech). Reactions were cycled as follows: 1 cycle of 95° for 2 min, 25 cycles of 95° for 30 sec, and 50°–55° for 40 sec. Reactions were stopped with 4 μl loading dye, containing 0.5% blue dextran and 99.5% formamide, and stored at −20°. Primer sequences, annealing temperatures, and extension nucleotide combinations used in each primer extension were as follows:

Atp7a: 5′-CTAACTATAGAGCTTGTTCTAAACT-3′; 50°; dCTP, dATP, ddTTP
Igf2 (CB6F1): 5′-CCATCGGGCAAGGGGATCTCAGCA-3′; 55°; dATP, dTTP, ddCTP, ddGTP
Igf2 (B6SpF1): 5′-AATTTTTAGATTATCAGTTATGGA-3′; 50°; dATP, dTTP, ddCTP, ddGTP

Extension products were resolved by 19% polyacrylamide gel electrophoresis on ALF*express* II (Amersham Pharmacia Biotech) automated sequencing systems. AlleleLinks software (v1.01) analyzed the CY-5 fluorescent signals captured during gel electrophoresis. The relative fluorescent signal for each of the two PE product peaks in a single lane was determined by assigning the largest peak the quantity of 10,000 and allowing the software to calculate the smaller peak quantity. Signal quantities were used to calculate the ratio of allelic transcripts in the original sample and are expressed as the quantity of the repressed allele/quantity of the active allele. Ratios from duplicate or triplicate PE reactions performed on each sample template were averaged to produce a mean expression ratio for each sample. The standard error of the mean (SEM) was calculated to describe the precision with which the triplicate reactions estimate the true mean expression ratio in each sample. The precision of a triplicate set of PE assays was expressed as a percentage of the mean: (SEM/mean) × 100.

The linear response range and allelic sensitivity of each PE assay were examined using a series of synthetic mixtures of the appropriate allelic templates. PCR was used to amplify large quantities of DNA fragments from the *Atp7a* and *Igf2* genes from individual mice homozygous or hemizygous for each alleleic haplotype assayed in the PE. PCR products from the same genomic DNA template were pooled and gel purified. DNA fragments were quantified by UV spectrophotometry and diluted to 50 ng/μl. Each allele was then serially diluted and mixed with the second allele to produce ratio mixtures of 1:1, 1:5, 1:10, 1:50, 1:100, 1:250, 1:500, and 1:1000. Each ratio mixture was used as a template in the PE assay.

Statistical analysis: The nonparametric Kruskal-Wallis ANOVA by ranks test was used to decide if differences between three or more cohorts were large enough to imply that the corresponding population means were different. When the Kruskal-Wallis test was significant ($P \leq 0.05$), the nonparametric Mann-Whitney *U*-test was used for pairwise comparisons of cohorts to determine which pairs were significantly different. Since the Mann-Whitney *U*-test generates unique ranks for the observations in each pairwise comparison, the false-positive error rate can be controlled per comparison (Lehmann 1988). The Spearmann rank-order test was used in all correlation analyses. Statistics and graphics were generated in Statistica (StatSoft).

RESULTS

Quantitative assays for allelic mRNA expression: A highly reproducible and precise measure of allelic mRNA species is necessary for examining gene expression from imprinted and X chromosomal loci. Of a variety of quantitative allelic assays currently in use, only primer-extension, also known as minisequencing, assays have been shown to be capable of achieving the relative quantitation of alleles in ratios of 1:100 or better (Singer-Sam *et al.* 1992; Greenwood and Burke 1996; Fahy *et al.* 1997). Primer-extension assays utilize PCR amplification for the generation of templates from small amounts of reverse-transcribed mRNA. A primer designed to anneal immediately 5′ of a sequence difference between two alleles is extended by a DNA polymerase, with nucleotide combinations selected to distinguish the two alleles (Figure 1). Sensitive quantification of the extension products is achieved by size separation (*e.g.*, electrophoresis) followed by detection of labeled extension products. In

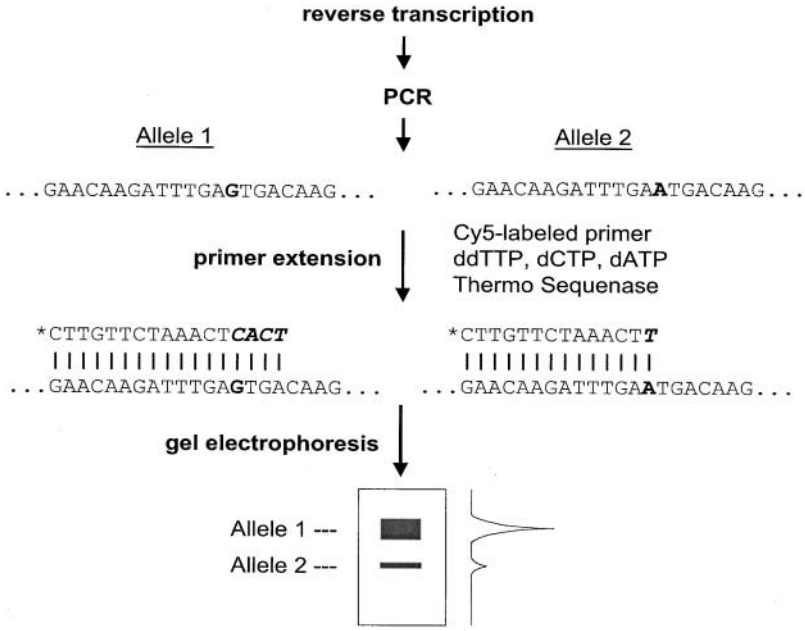

FIGURE 1.—Fluorescent PE assay for quantitative analysis of allelic gene expression. Total RNA is converted to cDNA in a reverse-transcription reaction and amplified by PCR with gene-specific primers flanking a region containing a sequence polymorphism. The PCR products derived from the two allelic transcripts are templates for the primer-extension reaction. A fluorescent-labeled primer anneals immediately 5′ of the single-base sequence difference. A combination of dideoxynucleotides and deoxynucleotides is used in the primer-extension reaction to produce two different-length extension products. Products are resolved by polyacrylamide gel electrophoresis and detected by an automated DNA sequencing system. The fluorescent signal peak for each extension product is quantified and used to calculate the ratio of expression of the two alleles in the original RNA sample. The extended products differ by three nucleotides and the transcript ratio of allele 1 to allele 2 is ~5:1.

this study, fluorescent primer-extension products are quantified and used to compute the relative ratio of expression of alleles in the original RNA samples. These primer-extension assays rely on the similar rates of reverse transcription and PCR amplification of the two alleles to generate templates whose relative concentrations accurately reflect the initial RNA sample. For both genes examined in this study, the equivalent amplification of the two allelic PCR products was extensively tested using purified allelic templates and synthetic mixtures of the templates, as has been performed with the SNuPE assay (SINGER-SAM *et al.* 1992; GREENWOOD and BURKE 1996). Optimization of the primer-extension procedure and automated gel scoring provided the high sensitivity (~1 part in 500) needed to detect age-associated changes in epigenetic control (Figure 2).

A PE assay was designed using a polymorphism in the expressed sequence of the X-linked ATPase copper-transporting type7a (*Atp7a*) gene. A standard curve of the *Atp7a* PE analysis on allelic ratio mixtures shows a linear range of allelic sensitivity between 1:1 and 1:1000 (Figure 2). The 1:1000 points are not reproducibly distinguishable from the assay background determined on the pure allele template. The precision of three repetitions of the PE assay across the range of the standard curve shows an average of 5.1%, with a range of 1.9–12.4%. The precision values of the mean expression ratio on duplicate reverse-transcription reactions performed on the same RNA were within 6% (data not shown). Likewise, the precision values of the mean expression ratio by triplicate PCR reactions performed on the same cDNA were within 3% (P. E. BENNETT-BAKER and J. WILKOWSKI, data not shown). The PE assay for the imprinted gene *Igf2* shows comparable levels of sensitivity and precision.

Age-associated loss of X inactivation in two experimental groups: Gene expression from the inactive X chromosome as a function of age was examined in three cohorts of T16H female mice (T16H++/++*Btk*$^{xid/J}$; abbreviated as J/X) at ages 2 months (n = 18), 13 months (n = 19), and 24 months (n = 16). Different-length primer-extension products distinguished *Atp7a* transcripts expressed from the active T16H X chromosome and the inactive X chromosome. Spleen and kidney RNA from each animal were reverse transcribed, and PCR amplified and analyzed for the ratio of allelic expression in triplicate PE reactions. In all animals, the dissected tissues showed no gross morphological changes or indications of overt tumors. The mean expression ratios of alleles from the inactive X chromosome (X_i) to the active X chromosome (X_a) were determined for each mouse in each J/X cohort group (Figure 3, A and B). Pairwise statistical comparisons of the cohorts yield P values <0.02 in all cases, confirming that each cohort has significantly different *Atp7a* allelic expression levels (Figure 4, A and B). In all comparisons, the older cohort has higher levels of expression from the inactive X chromosome than the corresponding younger cohort does. For the 13- and 24-month cohorts, there are no significant correlations in the activation status of *Atp7a* between spleen and kidney tissues derived from the same animal (13-month cohort, P = 0.286; 24-month cohort, P = 0.888).

A second population of female animals with the T16H translocation genotype (T16H++/++*Atp7a*$^{Mo\text{-}blo}$, abbreviated as T/M) was obtained and animals were sacrificed in age-matched cohorts. The *Atp7a* mRNA polymorphism found in J/X mice is also present in the T/M mice and distinguishes between transcripts expressed from the active T16H X chromosome and the inactive

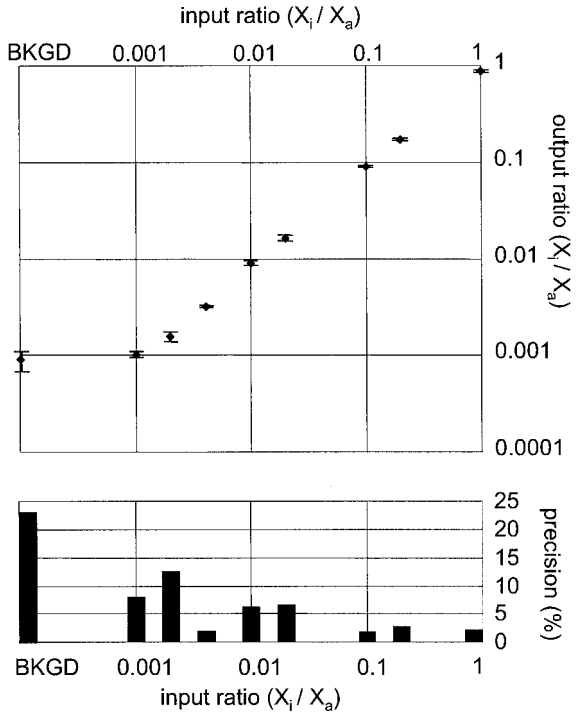

FIGURE 2.—Standard curve for the optimized *Atp7a* PE assay. (Top) The region of the standard curve for the *Atp7a* PE assay representing X inactivation in T16H++/++*Atp7a*$^{Mo\text{-}blo}$ female mice. Artificial mixtures of alleles from the ++*Atp7a*$^{Mo\text{-}blo}$ X chromosome (X_i) and the T16H++ X chromosome (X_a) were used to test the range of allelic sensitivity and precision of the *Atp7a* PE assay. The background (BKGD) value for the assay was determined on the pure T16H++ X chromosome allele. The diamonds represent the mean of triplicate PE assays performed on the same template mixture and the bars represent the SEM. (Bottom) The precision for each set of triplicate PE reactions on each input ratio mixture in percentages.

X chromosome. Twenty-seven female T/M mice were analyzed in four cohorts: 2 months ($n = 6$), 10 months ($n = 6$), 18 months ($n = 8$), and 24 months ($n = 7$). Kidney RNA was isolated from each animal and mean expression ratios (X_i/X_a) were determined by triplicate primer-extension assays (Figure 3C). In all animals, the dissected tissues showed no gross morphological changes or indications of overt tumors. The distributions of the expression ratios for each cohort support an age-associated loss of epigenetic silencing. Pairwise comparisons of the cohorts (Figure 4C) show mean expression levels significantly different between the 2-month cohort and the 10-, 18-, and 24-month cohorts. In addition, the 10-month cohort is significantly different from the 18-month cohort. In all comparisons of significantly different cohorts, the older cohort had higher levels of gene expression from the inactive X chromosome (Figure 4C).

Age-associated loss of genomic imprinting in two experimental groups: The autosomal imprinted locus *Igf2* was examined for loss of epigenetic maintenance in populations of age-matched animals. CB6F1 hybrid mice, offspring of BALB/cJ female × C57BL/6J male parents, were obtained and divided into male and female, "young," and "old" cohorts. The young cohorts were sacrificed as 15 males and 15 females at 2 months of age. The old cohorts were sacrificed as 15 males at 18 months and females at 23 months ($n = 13$), 18 months ($n = 1$), and 20 months ($n = 1$). Total tissue RNA was prepared from heart, kidney, and lung. Duplicate PE assays were performed on each sample to determine the allelic expression ratio of *Igf2* transcripts from the inactive allele, BALB/cJ, and the active allele, C57BL/6J. The population distributions of the expression ratios demonstrate tissue-specific and sex-specific activation patterns with age (Figure 5). With the exception of female kidney expression, each age-cohort comparison shows a higher level of the inactive allele at the older time point. Pairwise comparisons of young and old cohorts show a statistically significant and age-dependent increase in the expression of the inactive allele in heart and lung tissues. In kidney (Figure 5B) an increase in the expression of the repressed allele during aging is seen in the male CB6F1 samples; however, the effect occurs with a marginally significant P value ($P = 0.08$). The female CB6F1 kidney values differ significantly between the two age cohorts ($P < 1.0 \times 10^{-6}$), with a decrease in the expression of the repressed allele in the older cohort. However, the reactivation values for all of the female kidney samples are dramatically lower than those in any other tissue and approach the assay background levels. The age-associated change in the female cohort, therefore, is likely to be a reflection of fluctuations at the assay detection limit. There are no significant correlations in activation status of *Igf2* among heart, lung, and kidney tissues derived from the same animal, regardless of age (all comparisons; $P > 0.20$).

Last, a population of 64 C57BL6/J × *Mus spretus* F_1 interspecies hybrid females, ages 2–26 months, was available for further study of *Igf2* genomic imprinting status. Total RNA was prepared from heart, lung, and kidney tissue of each animal and examined for *Igf2* allelic ratios using the PE assay. In heart RNA, the population shows a significant correlation of expression from the inactive allele with animal age (Figure 6; $R = 0.3923$; $P = 0.00135$). A marginally significant age-associated loss of silencing of *Igf2* is also detected in lung ($R = 0.2497$; $P = 0.0431$). No significant age-associated correlation is observed in kidney RNA from the same animals.

DISCUSSION

The age-associated loss of silencing of the X-linked gene *Atp7a* is strongly supported by the experimental results. As expected, the inactive-X allele of *Atp7a* is repressed in young adult animals, with activity levels close to the background detection sensitivity of the PE assay (Figure 3, BKGD *vs.* 2-month cohort values;

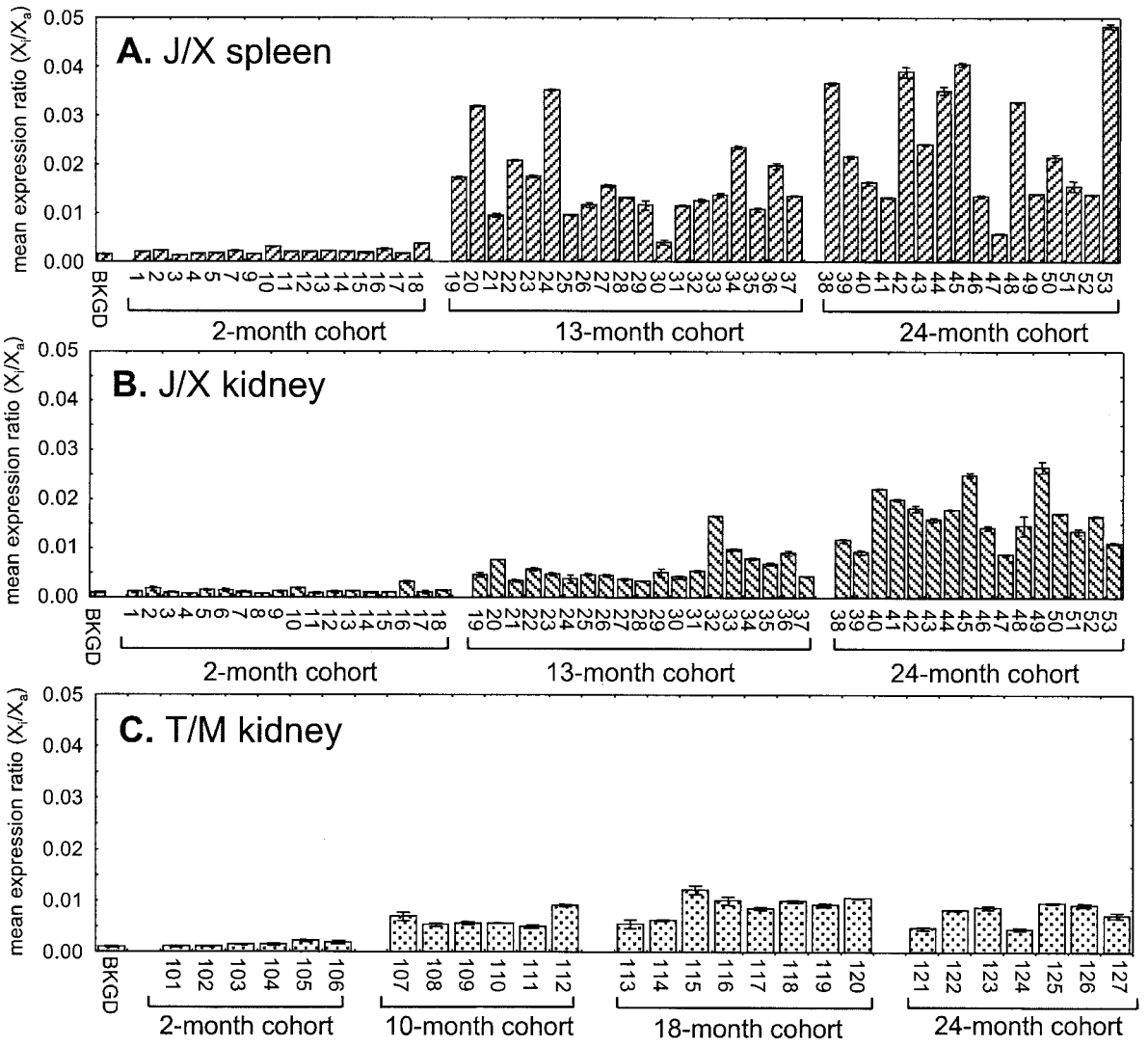

FIGURE 3.—Expression level of the inactivated allele of the X-linked gene *Atp7a* in two populations of mice. The T16H translocation was used to generate female mice with uniform inactivation of one X chromosome. The ratio of mRNA expression from the inactive-X allele to the active-X allele was determined by PE assay for each animal and tissue. Mice derived from the T16H stock J/X ($n = 53$) were killed in three age-matched cohorts and allelic *Atp7a* ratios were assayed from (A) spleen RNA and (B) kidney RNA. (C) Mice derived from the T16H stock T/M ($n = 27$) were killed in four age-matched cohorts, and allelic ratios were assayed from kidney RNA. For each animal and tissue the mean expression ratio of triplicate PE assays is shown (error bars indicate standard error of the mean). The background values (BKGD) indicate the mean expression ratio obtained from a male animal hemizygous for the active allele: (A) 0.0016, (B) 0.0011, and (C) 0.0009. Individual animal numbers are given on the *x*-axis.

EICHER 1970). The mean fraction of transcripts from the inactive-X chromosome rises from <0.3% for the 2-month cohort to 0.6–2.3% for the older cohorts. The highest single animal value for *Atp7a* loss of silencing, ~4.7%, appears in the 24-month cohort (Figure 3A, animal no. 53). The X activation pattern is consistent in both J/X tissues, with the 13-month population yielding a mean value intermediate between the 24-month and 2-month means, thereby supporting the likelihood of an age-dependent process. In addition, the loss of X inactivation in older animals is demonstrated in the separate mouse population, T/M.

Age-dependent loss of allelic repression is also observed at the imprinted locus *Igf2*; both tissue- and sex-specific effects are apparent (Figure 5). In most cases, the young animals are not fully repressed for the maternal *Igf2* allele, indicating a relaxed level of imprinting control, at least in these three tissues, by 2 months of age (CUI *et al.* 1998; JIANG *et al.* 1998). Heart- and lung-derived RNAs show the most consistent age-associated change, with similar results from males and females. In the older cohorts, the mean level of transcripts from the inactive allele ranged from 7.4 to 11.4% in these tissues. In contrast, the female kidney samples, at all

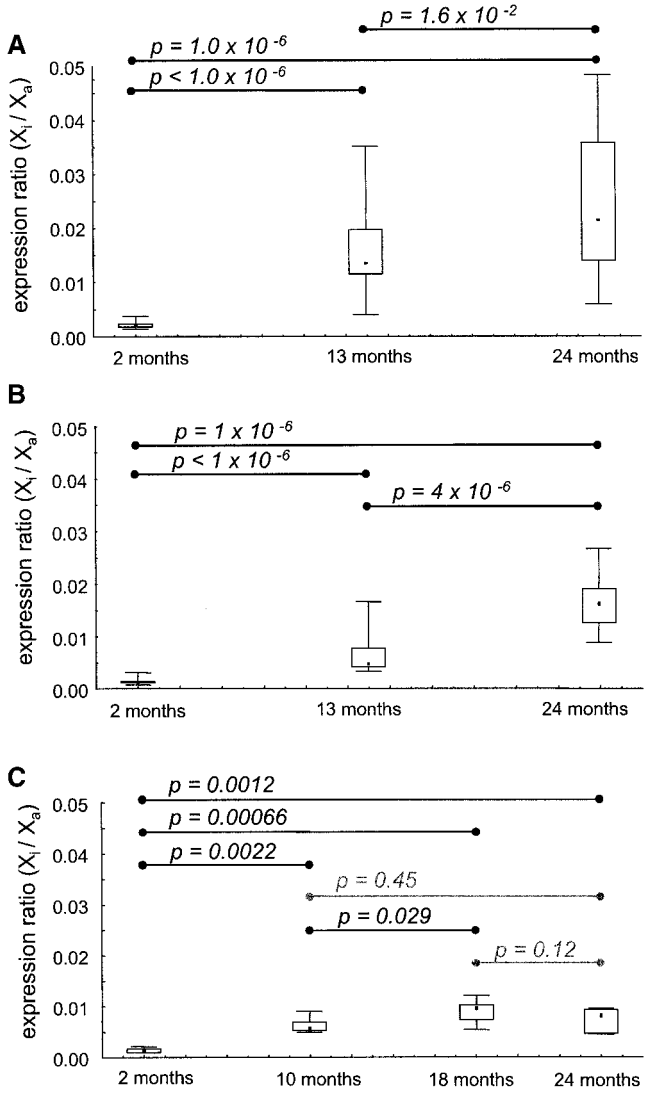

FIGURE 4.—Age-associated activation of the repressed *Atp7a* allele in T16H female mice. The expression ratio values for each cohort are summarized in box-plot format: median (dot), 25–75% values (open box), and minimum-maximum values (bars). Pairwise statistical comparisons of the cohort distributions are given as *P* values along the top of each display. The J/X female RNA expression ratios for spleen (A) and kidney (B) are shown. The cohort mean expression values for spleen are: 2-month cohort, 0.0022; 13-month, 0.0159; and 24-month, 0.0244. The cohort mean expression values for kidney are: 2-month cohort, 0.0013; 13-month, 0.0061; and 24-month, 0.0164. (C) The T/M females analyzed for RNA expression from kidney yielded the following mean expression ratios: 2-month cohort, 0.0015; 10-month, 0.0062; 18-month, 0.0090; and 24-month, 0.0074.

ages, remain tightly controlled for expression, with inactive-allele transcripts remaining essentially at the background detection level for the PE assay. In males, the *Igf2* kidney expression shows some increase in mean activation, but the difference is not statistically supported. Finally, the loss of stringent *Igf2* imprinting in heart and lung tissue is also confirmed from a second population of interspecies F_1 hybrid animals (Figure 6).

The absolute levels of expression from the inactive allele of *Igf2* are remarkably high in many of the cohorts in both young (2–3 months) and old (>18 months) animals. Mean levels of expression from the inactive allele ranged from ~6% (young CB6F1 animals) to 21% (old C57BL/6J × *M. spretus* animals). The exceptions to the large reactivation values are CB6F1 female kidney samples, with <1% expression from the inactive allele. The male and female CB6F1 kidney results were replicated in a second series of experiments on the same RNA samples (not shown); therefore, the unusually low female reactivation rates are unlikely to be simple assay error. With the existing data, it is unclear whether the differences in absolute reactivation result from strain-specific genetic variation, sex-specific gene expression, tissue-specific gene expression, or particular combinations of these effects. In addition, the overall high levels of reactivation from *Igf2* may be gene specific and may not be a general observation among imprinted genes. Additional work is in progress to distinguish these effects.

These experimental results extend and refine previous evidence for loss of epigenetic regulation during normal aging. Activation of an inactive-X gene was initially observed in adult T16H translocation mice at the level of cell-specific protein function (WAREHAM *et al.* 1987) or by observing progressive darkening of the coat during aging (CATTANACH 1974). In both earlier experiments, a wild-type allele was repressed on the inactive X, with a mutant allele on the active chromosome, thereby allowing the recovery of normal function to be readily observed. For the current study, either (i) both chromosomal *Atp7a* alleles are fully functional and produce normal wild-type product (J/X population) or (ii) the inactive X maintains a mutant allele with reduced function ($Atp7a^{Mo\text{-}blo}$, T/M population). In both cases, it is unlikely that activation of the repressed allele is driven by selection of cells with increased *Atp7a* function. The detection of this level of epigenetic change required molecular assay methods sensitive to allelic transcript ratios of 0.2% or less and statistical analysis of cohorts of animals. In the future, the examination of additional genes that are polymorphic between two X chromosomes should be able to address whether the silenced-X activation process occurs at individual loci or globally *in cis* across the inactive X.

For both X inactivation and genomic imprinting, populations of age-matched animals show consistent, although not identical, age-associated loss of epigenetic control. Similarly, different tissues from the same animals provide evidence for age-associated loss of gene silencing, independent of the cell-type-specific transcriptional controls. Therefore, the simple hypothesis—that epigenetic regulation of gene expression remains

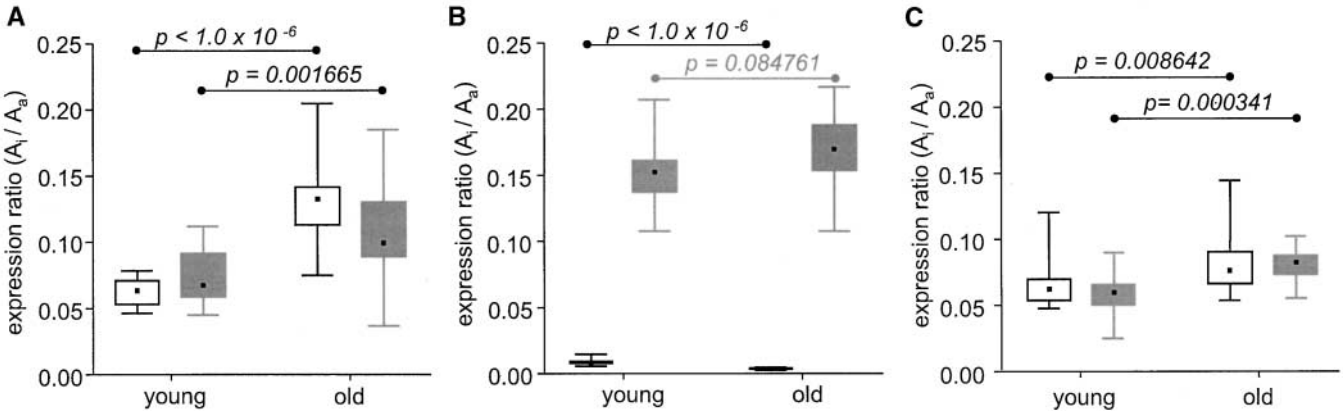

FIGURE 5.—Age-associated activation of the repressed *Igf2* allele in BALB/cJ × C57BL/6J F_1 hybrid male and female mice (CB6F1). The mean expression ratio of *Igf2* RNA transcripts derived from the inactive (BALB/cJ) and active (C57BL/6J) imprinted loci was determined for each animal tissue sample. The distribution of expression ratio values (BALB/cJ:C57BL/6J) for each cohort are provided as box plots with median (dot), 25–75% values (box), and minimum-maximum values (bars). Young and old male and female cohorts were analyzed for RNA expression ratios from (A) heart, (B) kidney, and (C) lung. The male distributions are shown with shaded boxes and the female distributions with open boxes. Pairwise statistical comparisons of the cohort distributions are given as *P* values along the top (solid lines, $P < 0.05$; shaded lines, $P < 0.1$). For each tissue, a mean *Igf2* assay background level of 0.0016 (±0.0004 SEM) was determined using mRNA from an animal homozygous for the C57BL/6J allele.

stable in normal tissues throughout life—is rejected. This implies that, for some genes at least, the developmentally programmed epigenetic state is subject to degradation or loss of specificity (CUTLER 1985; HOWARD 1996; JAZWINSKI 1996; VILLEPONTEAU 1997; FEINBERG 2001; JONES and TAKAI 2001). Quantitatively, this loss of epigenetic control may be at least one order of magnitude greater than previously determined somatic DNA mutation (*i.e.*, 10^{-2} *vs.* 10^{-4}; KING *et al.* 1994; MARTUS *et al.* 1995). Therefore, it is likely that epigenetic error is a common feature of normal aging cells. It is also possible that epigenetic loss of silencing may play a role in the progression of some cancers (FEINBERG 2001). The results of the current study, although simply a correlation between aging and loss of epigenetic control, are consistent with the established connection between aging and cancer.

What are the probable molecular targets of the observed loss of epigenetic control? Epigenetic errors may occur when chromatin modifications are not maintained accurately, and these alterations may accumulate over time or during mitotic cell divisions. Current knowledge of the chromatin basis of epigenetic information is incomplete, but includes (i) DNA methylation, (ii) covalent modification of histone proteins, (iii) heritable patterns of chromatin-associated proteins, and (iv) stable complexes of transcriptional control factors (LATHAM 1999; JENUWEIN and ALLIS 2001; JONES and TAKAI 2001). There is little evidence, at this time, to strongly link a specific form of epigenetic control with mamma-

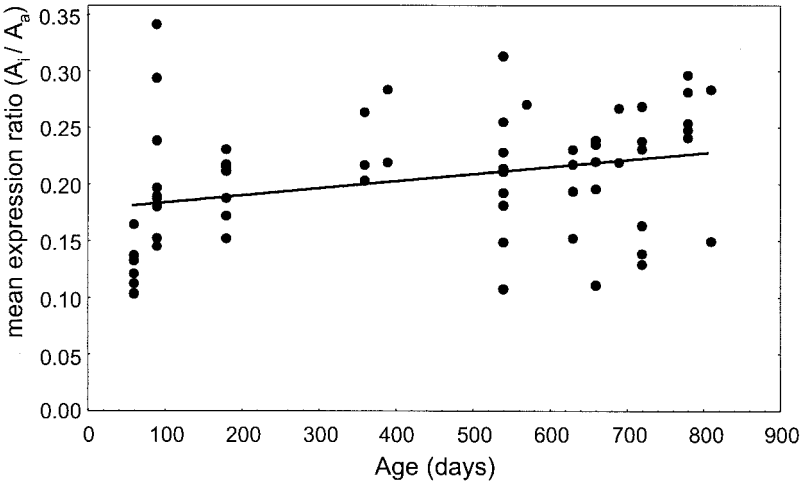

FIGURE 6.—Age-associated activation of the repressed *Igf2* allele in C57BL/6J × *M. spretus* F_1 hybrid female mice heart RNA. The expression ratio of *Igf2* RNA transcripts derived from the inactive (C57BL/6J) and active (*M. spretus*) imprinted loci were determined for each animal heart RNA sample. The population consisted of 64 F_1 hybrid animals with mean expression ratio values (C57BL/6J:*M. spretus*) for each animal displayed as a dot. Correlation analysis of age and expression ratio in the population using a Spearman rank-order test yielded $R = 0.3923$ and $P = 0.00135$. An *Igf2* PE assay background level of 0.0031 (±0.0007) was determined using mRNA from an animal homozygous for the active allele.

lian aging phenotypes. Future effort to uncover the molecular connection between the aging process and chromatin-level regulation will be essential, but will face the experimental challenge of variation among individuals. Regardless of the mechanism of chromatin-level control, our understanding of age-associated epigenetic dysfunction will benefit from accurate quantitative analysis and the examination of large numbers of normal, aging animals.

The authors acknowledge the work of Alex Greenwood and Michelle Southard-Smith in this project and the assistance of Roxanne Tavakkol and Corintha Goble. This work has been supported, in part, by grants from the National Institutes of Health (nos. AG11687 and AG16699) and the National Science Foundation (DBI-9629038). P.B.-B. was supported by National Institutes of Health predoctoral training grants GM07544-22 and AG00114.

LITERATURE CITED

Ausubel, F. M., R. Brent, R. E. Kingston, D. D. Moore, J. G. Seidman *et al.*, 1989 *Current Protocols in Molecular Biology*. John Wiley & Sons, New York.

Becksei, A., and L. Serrano, 2000 Engineering stability in gene networks by autoregulation. Nature **405:** 590–593.

Cattanach, B. M., 1974 Position effect variegation in the mouse. Genet. Res. **23:** 291–306.

Cui, H., I. L. Horon, R. Ohlsson, S. R. Hamilton and A. P. Feinberg, 1998 Loss of imprinting in normal tissue of colorectal cancer patients with microsatellite instability. Nat. Med. **4:** 1276–1280.

Cutler, R. G., 1985 Dysdifferentiative hypothesis of aging: a review, pp. 307–340 in *Molecular Biology of Aging: Gene Stability and Gene Expression*, edited by R. Sohal. Raven Press, New York.

Eicher, E. M., 1970 X-autosome translocations in mouse: total inactivation versus partial inactivation of the X-chromosome. Adv. Genet. **15:** 175–259.

Fahy, E., R. Nazarbaghi, M. Zomorrodi, C. Herrnstadt, W. D. Parker *et al.*, 1997 Multiplex fluorescence-based primer extension method for quantitative mutation analysis of mitochondrial DNA and its diagnostic application for Alzheimer's disease. Nucleic Acids Res. **25:** 3102–3109.

Feinberg, A. P., 2001 Cancer epigenetics takes center stage. Proc. Natl. Acad. Sci. USA **98:** 392–394.

Greenwood, A. D., and D. T. Burke, 1996 Single nucleotide primer extension: quantitative range, variability, and multiplex analysis. Genome Res. **6:** 336–348.

Hecker, K. H., and K. H. Roux, 1996 High and low annealing temperatures increase both specificity and yield in touchdown and stepdown PCR. Biotechniques **20:** 478–485.

Holliday, R., 1988 Toward a biological understanding of the ageing process. Perspect. Biol. Med. **32:** 109–123.

Howard, B. H., 1996 Replicative senescence: considerations relating to the stability of heterochromatin domains. Exp. Gerontol. **31:** 281–293.

Jazwinski, S. M., 1996 Longevity, genes, and aging. Science **273:** 54–59.

Jenuwein, T., and C. D. Allis, 2001 Translating the histone code. Science **293:** 1074–1080.

Jiang, S., M. A. Hemann, M. P. Lee and A. P. Feinberg, 1998 Strain-dependent developmental relaxation of imprinting of an endogenous mouse gene, *Kvlqt1*. Genomics **53:** 395–399.

Johnson, F. B., D. A. Sinclair and L. Guarente, 1999 Molecular biology of aging. Cell **96:** 291–302.

Jones, P. A., and D. Takai, 2001 The role of DNA methylation in mammalian epigenetics. Science **293:** 1068–1070.

King, C. M., E. S. Gillespie, P. G. McKenna and Y. A. Barnett, 1994 An investigation of mutation as a function of age in humans. Mutat. Res. **316:** 79–90.

Latham, K. E., 1999 Mechanisms and control of embryonic genome activation in mammalian embryos. Int. Rev. Cytol. **193:** 71–124.

Lehmann, E. L., 1988 *Nonparametrics: Statistical Methods Based on Rank*. Prentice-Hall, Upper Saddle River, NJ.

Lyon, M. F., 1999 Primer: X-chromosome inactivation. Curr. Biol. **9:** R235–R237.

Martus, H.-J., M. E. Dolle, J. A. Gossen, M. E. Boerrigter and J. Vijg, 1995 Use of transgenic mouse models for studying somatic mutations in aging. Mutat. Res. **338:** 203–213.

McAdams, H. H., and A. Arkin, 1999 It's a noisy business: genetic regulation at the nanomolar scale. Trends Genet. **15:** 65–69.

Singer-Sam, J., J. M. LeBon, A. Dai and A. D. Riggs, 1992 A sensitive, quantitative assay for measurement of allele-specific transcripts differing by a single nucleotide. PCR Methods Appl. **1:** 160–163.

Szilard, L., 1959 On the nature of the aging process. Proc. Natl. Acad. Sci. USA **45:** 35–45.

Villeponteau, B., 1997 The heterochromatin loss model of aging. Exp. Gerontol. **52:** 383–394.

Wareham, K. A., M. F. Lyon, P. H. Glenister and E. D. Williams, 1987 Age-related reactivation of an X-linked gene. Nature **327:** 725–727.

Weiler, K. S., and B. T. Wakimoto, 1995 Heterochromatin and gene expression in Drosophila. Annu. Rev. Genet. **29:** 577–605.

Wolf, R., and W. Jörn, 2001 Genomic imprinting: parental influence on the genome. Nat. Rev. Genet. **1:** 21–32.

Zhen, L., and R. T. Swank, 1993 A simple and high yield method for recovering DNA from agarose gels. Biotechniques **14:** 894–898.

Communicating editor: L. Pillus